IEEE Access
Multidisciplinary | Rapid Review | Open Access Journal

Received June 26, 2020, accepted July 14, 2020, date of publication July 24, 2020, date of current version August 4, 2020.

Digital Object Identifier 10.1109/ACCESS.2020.3011697

Human Posture Recognition Using a Hybrid of Fuzzy Logic and Machine Learning Approaches

WEIYAN REN[1], (Graduate Student Member, IEEE), OU MA[2], HONGXIN JI[1], AND XINYUAN LIU[3], (Member, IEEE)

[1]School of Aerospace Engineering, Tsinghua University, Beijing 100084, China
[2]College of Engineering and Engineering Sciences, University of Cincinnati, Cincinnati, OH 45221, USA
[3]Rehabilitation Medicine Department, China-Japan Friendship Hospital, Beijing 100029, China

Corresponding author: Weiyan Ren (rwy17@mails.tsinghua.edu.cn)

This work was supported in part by the China Manned Space Engineering Office (Astronaut rehabilitation training) under Project 020201, and in part by the Tsinghua University through internal research and development funds.

ABSTRACT An autonomous assistive robot needs to recognize the body-limb posture of the person being assisted while he/she is lying in a bed to provide care services such as helping change the posture of the person or carrying him/her from the bed to a wheelchair. This paper presents a data-efficient classification of human postures when lying in a bed using a hybrid fuzzy logic and machine learning approach. The classifier was trained using a relatively small dataset containing 19,800 annotated depth images collected using Kinect from 32 test subjects lying in bed. An overall accuracy of 97.1% was achieved on the dataset. Furthermore, the image dataset including depth and red-green-blue (RGB) images, is available to the research community with the publication of this paper, with the hope that it can benefit other researchers.

INDEX TERMS Human posture, posture recognition, lying in bed, human posture dataset.

I. INTRODUCTION

As the world's population ages and the workforce population decreases, there is an urgent need to advance automation and robotics technology to help healthcare workers with the increase in labor-intensive assistive needs [1]–[4]. Researchers have found that a lack of technology maturity in terms of safety and comfort is impeding the healthcare applications of assistive robots [5]. The motion trajectories of an assistive robot's arms are a critical factor affecting the safety and comfort of the person receiving assistance [6]. The relative position and posture of the human body in bed are the main input parameters for the robot's motion trajectory planning. Accurate and efficient recognition of the patient's lying posture are the key inputs for dual-arm assistive robots to ensure the safety and comfort of the service. In addition, the sleeping posture is an important parameter relating to human health; poor posture can cause pain and may lead to disease and other complications, such as sleep apnea and pressure ulcers. Therefore, the accurate recognition of lying postures is of great importance to the healthcare service of patients lying in bed [7].

To date, there have been few studies that focus on the recognition of human lying postures. There have been two categories of recognition methods: 1) those based on pressure mapping (PM) and 2) those based on visual imaging. PM methods collect data via sensors placed beneath the body of a patient and use the pressure distribution data to identify a person's sleeping posture and to determine where the limbs touch the bed; these methods can recognize three main stable sleeping postures with an accuracy rate of 91.2% [8]. In subsequent research, the PM system has been used to create a time-stamped and whole-body pressure map of patients for bed posture classification and limb identification [9]. In [10], the research team used a binary pattern matching metric to develop a high-performance 8-posture classifier. In [11], based on the PM dataset, the team used a deep convolutional neural network (DCNN) to recognize lying postures with an accuracy of 98%. Based on the bed-sheet pressure sensor data in [12], the researchers used an artificial neural network to identify three types of in-bed poses (supine, prone and left and right lateral). Harada *et al.* [13] compared the measurement data of a pressure sensing mattress to a synthetic database that was precomputed by estimating the pressure distribution of a kinematic model. Grimm *et al.* [14] presented a system to automatically estimate the body posture of a reclined patient using measurement data from a pressure sensing mattress and

The associate editor coordinating the review of this manuscript and approving it for publication was Ehsan Asadi.

identified the human orientation and pose using a skeleton model. Clever *et al.* [15] presented two convolutional neural networks to estimate the three-dimensional (3D) joint positions of a person in a configurable bed from a single pressure image. In later work, Kapusta *et al.* [16] motivated the robots to configurations optimized for the tasks by estimating the patient's pose using a pressure sensing mat. Casas *et al.* [17] presented a deep learning method to retrieve 3D human poses from pressure sensor data by regression. Hsia *et al.* [18] presented a two-level data fusion architecture of a pressure sensitive bed system and evaluated the pressure sensor layouts and posture classification algorithms. Liu *et al.* [19] developed a novel framework for pressure image analysis to monitor sleep postures, including a set of geometrical features for sleep posture characterization and three sparse classifiers for posture recognition.

Although PM-based method can contribute to the recognition of human postures, the PM sensors are expensive and require frequent maintenance, which hinder large-scale applications. In addition, inertial sensors, such as accelerometers, magnetometers, wireless devices, and gyroscopes, are also used for lying posture recognition [20], [21]. This technique requires the users to wear sensors on their bodies, which can be uncomfortable or burdensome [19].

Recently, visual-based methods have gained momentum. In [22], computer vision was used to detect particularly sparse actions such as getting in or out of a bed. In [23], random forests were applied to a large nonpublic synthetic dataset of depth frames to capture a diverse range of human shapes. In [24], a motion capture system was introduced for 3D human posture recognition; however, the experimental settings had not been determined in practical applications. In [25], a method was introduced to collect the position data of a human body and head; these data were then applied to measure breathing movements and recognize sleeping postures. A near-infrared modality was employed in [26] for long-term monitoring in full darkness, achieving in-bed pose estimation with patients covered in sheets or blankets. Huang *et al.* [27] proposed a multimodal approach to human sleeping posture classification using a pressure sensor array and a video camera as complementary modalities for feature extraction and classification. Kuo *et al.* [28] proposed an image-based solution to recognize the sleep direction using an infrared radiation-based night vision camera to capture video frames while patients sleep. Although there are many vision-based methods to identify human posture, few studies have focused on the posture of humans lying in bed [21], [29], [30]. Due to different application areas, previous research has mainly focused on coarse-grained lying posture classification.

All the learning-based methods rely on available data for training. To the best of our knowledge, the existing publicly available datasets of human lying postures, include the PM dataset [8], the 3D posture and pressure mat dataset [15], and the simultaneously collected multimodal lying pose (SLP) dataset [26]. The PM dataset includes pressure distribution data collected using pressure sensor mats placed beneath the bodies of participants. It has been used for detecting and correcting improper sleeping in patients for the prevention of pressure induced ulcers [8]. The 3D posture and pressure mat dataset consists of over 28,000 pressure images from 17 human participants. The 3D human posture was estimated on a configurable bed based on this dataset [15]. The dataset contains some challenging scenarios, such as when the bed and human are configured in a seated posture and when limbs are raised off the pressure sensing mat. The SLP dataset [26] was obtained through thermal diffusion based on long wavelength infrared ray technology with participants lying in bed in three different body postures and covered by sheets or blankets. However, the currently available in-bed datasets lack fine-grained lying postures.

There are two key steps in accurately recognizing a fine-grained human lying posture: (1) creating a dataset of human in-bed images with various possible body postures and (2) developing a posture recognition tool. In this paper, we present our research for these two steps.

In this research, we created a dataset of images of humans lying in bed and developed a hybrid fuzzy logic and support vector machine (SVM) algorithm to recognize the correct posture from 20 possible lying postures. A state-of-the-art result was achieved with our dataset. Compared with the currently available lying posture classification methods, the proposed method along with our dataset can achieve fine-grained posture recognition. The main contributions of our study include a dataset of depth and RGB images of humans lying in bed in 20 distinguished body postures, which we have created and are releasing to the research community, and a data-efficient posture classification method based on a hybrid fuzzy logic and SVM approach.

II. THE PROPOSED APPROACH

The structure of the human body is complex, and there can be numerous different postures while lying in bed. Therefore, it can be overdemanding to annotate all possible postures, especially fine-grained postures, while training and testing. The method proposed in our study is the first to recognize the postures of different body segments, from which the whole-body fine-grained posture is then identified. Fuzzy logic possesses advantages in the fuzzy comprehensive judgment of an unknown or uncertain description of a complex dynamic system or control system with strong nonlinear characteristics [31], [32]. Moreover, human limbs (such as the upper limbs) feature various degrees of freedom (DOFs) of the joints; they are flexible, have complex structures, and have diverse and uncertain motions. It is difficult to describe and recognize the posture of human limbs through rigorous mathematical modeling [33]. We therefore utilize fuzzy logic to recognize the limb postures.

The architecture of the approach is shown in Fig. 1. First, based on the statistics of the different lying postures of a participant, we collected the image data of limb postures and whole-body lying postures. Second, a fuzzy rule base

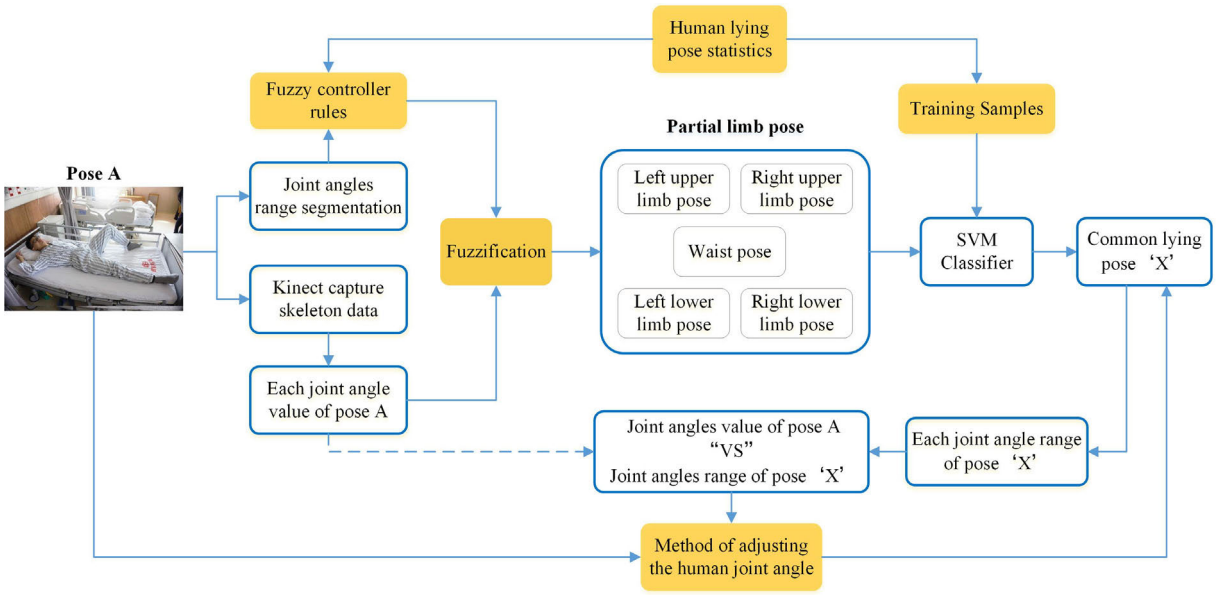

FIGURE 1. Whole-body lying posture recognition procedure.

was obtained through statistical analysis of the limb posture dataset. We then used the rule base to fuzzy the joint motion and, thereby obtained a relational model between the joint motion and the limb postures. In this way, we were able to recognize limb postures through fuzzy recognition. Finally, by marking the limb postures and the whole-body lying postures, the lying posture dataset of the human body was established. The dataset provides training samples for the classifier model in the machine learning process, and the classifier was trained with those samples to obtain the relational model between the limb postures and the whole-body lying postures. Thus, an SVM algorithm can recognize a whole-body lying posture.

III. LIMB POSTURE RECOGNITION

A. STATISTICAL ANALYSIS

1) STATISTICAL ANALYSIS OF LIMB POSTURES AND LYING POSTURES

Usually, when a person's lying posture or joint angles change significantly, it is necessary to adjust the trajectories of the robotic arms. However, due to the robot's redundant DOFs, the calculation of the trajectories takes time [34]. Therefore, it is difficult to calculate the dual-arm trajectory in real time as the human lying posture changes. However, to improve the ergonomics of human-robot interactions, we need to use an optimal dual-arm trajectory to complete each holding process. To solve this problem, we collected the patient's common lying postures from a large number of samples and precalculated the corresponding motion trajectories of a robot from those postures.

Therefore, we collected statistical data of lying postures from hospital patients. The requirements of the data collection are as follows:

(1) Patients who are unconscious or lying in a single posture are excluded.

(2) Patients who are overweight and likely to have limited lying postures are excluded.

(3) Children whose height is less than 1 meter are excluded.

(4) Lying postures at different times of the day are included.

Statistical analysis of the abovementioned requirements enabled us to collect 1800 valid lying postures. Through the analysis of the data, similar lying postures were statistically categorized into 20 common lying postures, as shown in Fig. 2. Through the classification of similar limb postures, we determined 9 common postures of the upper limbs (both left and right upper limbs) and 9 common postures of the lower limbs (both left and right lower limbs).

2) MOTION STATISTICS AND ANALYSIS OF HUMAN JOINTS

The human body is a complex multibody system consisting of approximately 206 bones, including the skull, trunk bones, and limb bones [35]. The limb bones are composed of upper and lower limb bones, which are the main contributors to human motion. In this work, we simplified the information of human bones by dividing an upper limb into 6 segments: the upper arm, the lower arm, the palm, the shoulder joint connecting the upper arm and the torso, the elbow joint connecting the upper arm and the lower arm, and the wrist joint connecting the lower arm and the palm. Similarly, the lower limb is divided into 7 segments: the thigh, the calf, the foot, the hip joint connecting the thigh and the torso, the knee joint connecting the thigh and the calf, the ankle joint connecting the calf and the foot, and the waist part between the hip and the rib. The motions of the upper limbs, lower limbs, and waist are the most complex parts of the whole-body motion.

FIGURE 2. Common lying postures from the statistical analysis. Through the statistical analysis of a large amount of lying data, we have summarized 20 lying postures that are the most common for humans lying in bed.

Because the palm and foot are located at the ends of the limbs, they have little influence on the whole-body posture. Hence, postures of the palms and the feet are not included in this study.

Through the statistical analysis of the range of motion of a human limb based on anatomical knowledge, we use the limb joint angles to describe the motions of individual limbs in detail. Taking the left upper limb as an example, the shoulder joint has 3 DOFs, referring to bending and stretching, abduction, and rotation of the upper arm, as defined by α_1, α_2, and α_3, respectively, which indicate the posture of the upper arm in the sagittal plane and the lateral plane and the rotation angle of the arm on its own axis. We define the elbow joint angle by α_4, denoting the angle between the upper arm and the forearm (lower arm). Similar to the upper limb, the hip joint has 3 DOFs, the knee joint has 1 DOF, and the waist has 1 DOF. The angular ranges of the DOFs of the limb joints are shown in Table 1.

B. CALCULATION OF THE JOINT ANGLES

Based on Kinect's depth images of a human body and the information from the human skeleton, we collected 3D coordinate data using a C++ program and Kinect equipment for Windows SDK. We then calculated the joint angles via the space vector method. As an example, we show the calculation of the joint angles for the left upper limb (shown in Fig. 3). We utilized the 3D coordinate data of the head, the left shoulder (LS), the right shoulder (RS), the left elbow (LE), and the left wrist (LW) to calculate the joint angles of the left upper limb.

In the motion analysis of the left shoulder, the human body coordinate system is established with the left shoulder joint

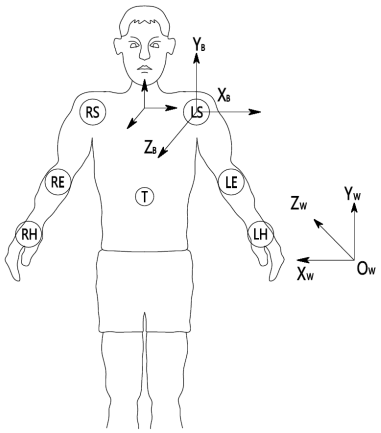

FIGURE 3. Human body coordinate system.

P_{LS} as the origin O_B, the direction vector $P_{RS}P_{LS}$ from the LS to the RS as the positive direction of the *x-axis*, the direction vector P_TP_N from the body to the midpoint of both shoulders as the positive direction of the *y-axis*, and the cross product of the *x-* and *y-axes*, i.e., $P_{RS}P_{LS} \times P_TP_N$, as the positive direction of the *z-axis*.

The 3D coordinates ${}^WP_i$ in the Kinect coordinate frame C_W can be transformed into the coordinates ${}^BP_i$ in the human body system C_B. For example, the coordinates of the elbow joint in C_B are denoted as:

$$ {}^Bp_{LE} = \begin{bmatrix} {}^Bp_{LE}|x \\ {}^Bp_{LE}|y \\ {}^Bp_{LE}|z \end{bmatrix} \tag{1} $$

As described in Section 2.2, the joint angles of the shoulder are denoted as α_1, α_2, and α_3, and the joint angle of the elbow

TABLE 1. Angular ranges of the degrees of freedom of the limb joints.

Limbs	Shoulder Joint			Elbow Joint	Waist	Hip Joint			Knee Joint
	α_1 [°]	α_2 [°]	α_3 [°]	α_4 [°]	μ [°]	β_1 [°]	β_2 [°]	β_3 [°]	β_4 [°]
Upper limb	0~180	0~180	-60~90	0~150					
Waist					0~60				
Lower limb						0~90	0~90	-60~90	0~150

is denoted as α_4. The angle of the upper arm in the horizontal direction is expressed as follows:

$$\alpha_1 = \begin{cases} \arctan \dfrac{{}^{B}p_{LE}|x}{{}^{B}p_{LE}|z} & {}^{B}p_{LE}|z \neq 0 \\ \pm\dfrac{\pi}{2} & {}^{B}p_{LE}|z = 0 \end{cases} \tag{2}$$

The formula of the movement angle α_2 of the upper arm in the vertical direction is expressed as follows:

$$\alpha_2 = \arccos \frac{{}^{B}p_{LE}|y}{|O_B{}^{B}p_{LE}|} \tag{3}$$

The rotation angle α_3 of the arm on its own axis is decided by the normal vector of the vertical plane as well as the normal vector of the plane of the upper arm and the forearm, as follows:

$$\alpha_3 = \arccos\left(\frac{Y_B \times O_B{}^{B}p_{LE}}{|O_B{}^{B}p_{LE}|} \cdot \frac{O_B{}^{B}p_{LE} \times {}^{B}p_{LE}{}^{B}p_{LH}}{|O_B{}^{B}p_{LE}| \cdot |{}^{B}p_{LE}{}^{B}p_{LH}|}\right) \tag{4}$$

The joint angle α_4 of the elbow motion, i.e., the angle between the upper arm and forearm can be calculated via the vector of the upper arm $O_B{}^{B}p_{LE}$ and the vector of the forearm as follows:

$$\alpha_4 = \arccos \frac{O_B{}^{B}p_{LE} \cdot {}^{B}p_{LE}{}^{B}p_{LH}}{|O_B{}^{B}p_{LE}| \cdot |{}^{B}p_{LE}{}^{B}p_{LH}|} \tag{5}$$

In this work, we used degrees as the angular unit instead of radians for a more intuitive view. The calculations of the other body segments is similarly defined and is thus, not repeated here.

C. FUZZY PROCESS

The fuzzy logic process consists of three steps: fuzzification, fuzzy reasoning, and defuzzification. As shown in Fig. 4, the fuzzy rules and reasoning, as the core steps in the process, can make decisions on the basis of the fuzzy logic rules. Figure 4 shows the fuzzy process of recognizing the left upper limb posture. Based on the ranges of the limb motions and joint angles, the fuzzy rules are established via the fuzzification of the joint angles and the analysis of the dataset. Hence, a limb posture can be recognized through this process.

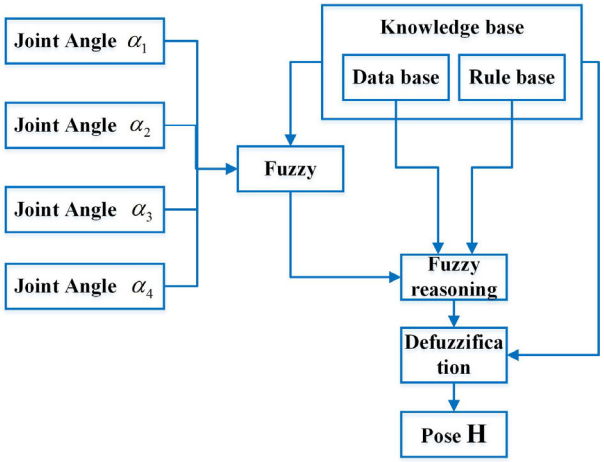

FIGURE 4. Fuzzy logic process for recognizing the upper limb posture.

1) FUZZIFICATION

To establish the fuzzy rules, we made a detailed segmentation of the ranges of the joints angles. Specifically, a complete motion of the limb in one DOF is decomposed into several small motions. Again, the left upper limb is taken as an example to explain the fuzzification.

The angle range of α_1 is uniformly quantized to the range of [0, 8]. The domain of α_1 is [0, 2, 4, 6, 8], and the corresponding fuzzy set is α_1 = {VO, VS, S, VM, VB}. The quantized range and domain of α_2 are the same as those of α_1, and the corresponding fuzzy set is α_2 ={RO, RC, C, F, RF}. The angle range of α_3 is uniformly quantized to the range of [−4, 4]. The domain of α_3 is [−4, 0, 4], and the corresponding fuzzy set is α_3 = {NB, ZO, PB}. The angle range of α_4 is nonuniformly quantized to the range of [0, 4] (i.e., to quantize within the range of [0°, 150°], the range is quantized as 0 when $\alpha_4 < 10°$ and as 4 when $\alpha_4 > 90°$). The domain of α_4 is [0, 2, 4], and the corresponding fuzzy set is α_4 = {EO, EM, EB}. Based on the motion space range of the left upper arm, its posture is denoted as the output set: H = [LUO, LUT, LUH, LUF, LUI, LUS, LUE, LUG, LUN]. The set H represents the following 9 left upper limb postures obtained through fuzzification.

TABLE 2. The fuzzy rules for recognizing the left upper limb posture.

		VO			VS			S			VM			VB		
		ZO	PB	NB	ZO	PB	NB	ZO	PB	NB	ZO	PB	NB	ZO	PB	NB
RO	EO	LUO	LUO	LUO	LUO	LUO	LUH	LUO	LUO	LUH	LUH	LUH	LUH	LUH	LUH	LUH
	EM	LUO	LUE	LUG	LUN	LUE	LUG	LUN	LUE	LUG	LUH	LUE	LUG	LUH	LUE	LUG
	EB	LUN	LUI	LUS	LUN	LUI	LUS	LUN	LUI	LUS	LUN	LUI	LUS	LUN	LUI	LUS
RC	EO	LUO	LUO	LUO	LUF	LUF	LUF	LUF	LUF	LUF	LUH	LUH	LUH	LUH	LUH	LUH
	EM	LUO	LUE	LUG	LUF	LUF	LUF	LUF	LUF	LUF	LUH	LUE	LUG	LUH	LUE	LUG
	EB	LUN	LUI	LUS	LUF	LUF	LUF	LUF	LUF	LUF	LUN	LUI	LUS	LUN	LUI	LUS
C	EO	LUO	LUO	LUO	LUF	LUF	LUF	LUF	LUF	LUF	LUH	LUH	LUH	LUH	LUH	LUH
	EM	LUO	LUE	LUG	LUF	LUF	LUF	LUF	LUF	LUF	LUH	LUE	LUG	LUH	LUE	LUG
	EB	LUN	LUI	LUS	LUF	LUF	LUF	LUF	LUF	LUF	LUN	LUI	LUS	LUN	LUI	LUS
F	EO	LUT	LUT	LUT	LUT	LUT	LUT	LUT	LUT	LUT	LUI	LUI	LUI	LUI	LUS	LUS
	EM	LUT	LUE	LUG	LUT	LUE	LUG	LUT	LUE	LUG	LUI	LUI	LUI	LUI	LUS	LUS
	EB	LUN	LUI	LUS	LUN	LUI	LUS	LUN	LUI	LUS	LUI	LUI	LUI	LUI	LUS	LUS
RF	EO	LUT	LUT	LUT	LUT	LUT	LUT	LUT	LUT	LUT	LUI	LUI	LUI	LUI	LUS	LUS
	EM	LUT	LUE	LUG	LUT	LUE	LUG	LUT	LUE	LUG	LUS	LUS	LUS	LUS	LUS	LUS
	EB	LUN	LUI	LUS	LUN	LUI	LUS	LUN	LUI	LUS	LUS	LUS	LUS	LUS	LUS	LUS

(1) LUO stands for the original posture (the natural straightening state of the left upper limb near the body).

(2) LUT stands for the left upper limb lifting upwards by a large extent (forearm not bent).

(3) LUH stands for the left upper limb extending outwards by a large extent (forearm not bent).

(4) LUF stands for the left upper limb in 3D space.

(5) LUI stands for the left upper limb extending and lifting slightly outwards with the forearm bent and rotated.

(6) LUS stands for the left upper limb extending and lifting by a large extent with the forearm bent and rotated.

(7) LUE stands for the left upper limb extending slightly, lifting by a large extent with the forearm bent and rotated inward.

(8) LUG stands for the left upper limb extending by a large extent, lifting slightly, with the forearm bent slightly and rotated outward.

(9) LUN stands for the left upper limb extending by a large extent, lifting slightly, with the forearm bent by a large extent and rotated outward.

2) KNOWLEDGE BASE

The knowledge base is mainly composed of two parts: the dataset and the rule base. The dataset includes membership functions for each linguistic variable, scale transformation factors, and grading numbers of the fuzzy variables. The rule base includes a series of judgment rules expressed by fuzzy linguistic variables and is composed of the sum of several fuzzy "if-then" statements.

The fuzzification method employed in this study is a Gaussian membership function, and its mathematical model is defined as follows:

$$\mu(x) = \exp\left[\frac{-(x-c)^2}{\sigma^2}\right] \tag{6}$$

where c and σ are the mean and offset of the Gaussian membership function, respectively.

In the case of the left upper limb, the fuzzy model has 4 inputs and 9 outputs, which represent the 4 DOFs and the 9 postures of the left upper limb, respectively. The fuzzy logic rules are usually expressed by the following fuzzy statement:

$$\text{If } \alpha_1 \text{ and } \alpha_2 \text{ and } \alpha_3 \text{ and } \alpha_4 \text{ then H.} \tag{7}$$

Based on the statistical dataset of the limb posture in Chapter III and the common limb posture obtained by statistics, the rules of the fuzzy process for recognizing the limb posture are shown in Table 2.

3) FUZZY REASONING AND DEFUZZIFICATION

Fuzzy reasoning and defuzzification are important steps in a fuzzy process. The reasoning step is based on the implicit relations and inference rules in the fuzzy logic process. Based on the input of the fuzzy system and the rules, and through logical operations such as fuzzy relation synthesis and fuzzy inference synthesis, the reasoning step deduces a certain conclusion from some fuzzy preconditions and, thereby obtains the output of the fuzzy process [32]. In this study, the Mamdani method is used for fuzzy reasoning because Mamdani fuzzy inference rules conform to human habits of thinking and expression and are thus more suitable for the logical expression of this research problem.

Defuzzification can be done using a few different methods. We adopt the commonly used center of gravity method (centroid method) [36], which is expressed as

$$\alpha_0 = \frac{\int \alpha_l \cdot \mu_l(a)\, da}{\int \mu_l(a)\, da} \tag{8}$$

where α_0 is the value obtained by the centroid method; $\int \mu_l(a)\, da$ is the integration of the membership degree of all

elements of the fuzzy logic at the output over the continuous domain; and α_l represents the output angle corresponding to the largest value of the membership function which corresponds to each fuzzy subset of the output.

D. LIMB POSTURE RECOGNITION

Based on the Kinect depth images of the human body and the proposed method, we can recognize the static and dynamic postures of limbs. For the real-time recognition of a dynamic body posture, the motion definition of the left upper limb is as follows. The left upper limb naturally moves from the upside posture to the on-abdomen posture. The corresponding motion sequence is shown as a series of video snapshots in Fig. 5.

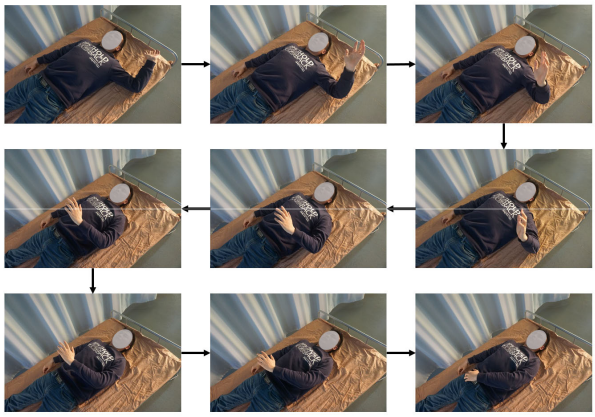

FIGURE 5. Snapshots of the left upper limb motion.

In this video, as the left upper limb moves, 3 postures of the left upper limb are recognized, as shown in Fig. 6. By comparing the limb postures in the video, it can be seen that the method can accurately recognize the limb postures.

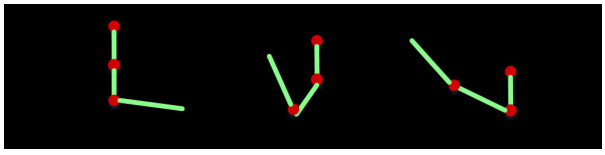

FIGURE 6. Dynamic recognition of the limb postures.

Similar to the real-time recognition of the left upper limb, postures of the right upper limb, the left lower limb, and the right lower limb (9 postures each) are obtained by the fuzzy logic process. It is worth noting that the factors considered when designing the fuzzy rules for the lower limbs were slightly different from those of the upper limbs because as the human body lies down, the flexion of the lower leg is constrained by the extension of the upper leg, and in its natural state, the flexion angle of the lower leg is related to the extension angle of the upper leg. Therefore, in the definition of fuzzy rules, the flexion angle of the lower leg is nonlinearly related to the extension angle of the upper leg.

In this section, we have shown that with prior knowledge and practice, we can recognize the postures of the limbs using the fuzzy logic process. The body postures are composed of the postures of the limbs, and the postures of the limbs are the basis for recognizing the whole-body posture. In Section IV, the classifier is trained using the limb posture data to recognize the whole-body lying posture.

IV. LYING POSTURE RECOGNITION

The whole-body lying posture recognition method proposed in this study can be divided into three parts: (1) human joint coordinate extraction, joint angle calculation, and segmentation; (2) fuzzification and sample labeling; and (3) classifier training and lying posture recognition. Among the three parts, it is important to choose an appropriate method for training and classification based on the characters of the sample data or the extracted features. The existing classification methods fall into three major categories: semantic description, state-space modeling and model-based matching [31]. Commonly used state-space models include the hidden Markov model (HMM), the dynamic Bayesian network (DBN), artificial neural networks (ANNs), and SVM. SVM is a simple classification method based on statistical learning theory, which falls into the supervised learning methodology in the machine learning domain. It enhances the generalization performance and solves the problems of small sample space and nonlinearity. The method has been widely applied in many fields, such as text training, gait recognition, and data mining. [37]. We chose the SVM method because it is simple and applicable. The other classification methods may also be appropriate; however, a comparative study of these applicable machine learning methods for the problem at hand is not the focus of this paper.

A. RECOGNITION METHOD

The multiclass SVM was chosen to recognize patient lying postures. At present, the multiclass SVM can be performed using several different methods [38]. Considering that the number of posture types in this work is not particularly large, this work is capable of forming a multiclass SVM classifier based on the one-to-one voting strategy. The flow chart of the lying posture recognition algorithm is shown in Fig. 7.

The posture recognition problem in this work is a nonlinear classification problem, and the SVM method applied in this work has unparalleled advantages. The principle of the SVM algorithm is described below. First, we set up a dataset as follows:

$$\left\{\left(\overrightarrow{x_1}, y_1\right), \left(\overrightarrow{x_2}, y_2\right) \cdots, \left(\overrightarrow{x_n}, y_n\right)\right\} \tag{9}$$

where $\overrightarrow{x}$ is the two-dimensional (2D) sample feature vector. In this case, the sample is linearly inseparable, and the classification function is as follows:

$$f(x) = \sum y_i a_i K(x \cdot x_i) + b' \tag{10}$$

where $a = (a_1, \cdots, a_n)$ is the Lagrange multiplier; K is the kernel function; and b' is the optimal hyperplane offset.

TABLE 3. Training samples of the SVM classifier.

Lying Posture	Local Limb Posture				
	Left upper limb	Right upper limb	Waist	Left lower limb	Right lower limb
Posture1	LUO	RUF	WON	LSE	RFO
Posture1	LUT	RUS	WON	LNI	RFI
⋮	⋮	⋮	⋮	⋮	⋮
Posture20	LUG	RUF	WTW	LTH	RSI
Posture20	LUN	RUF	WTW	LFO	RSE

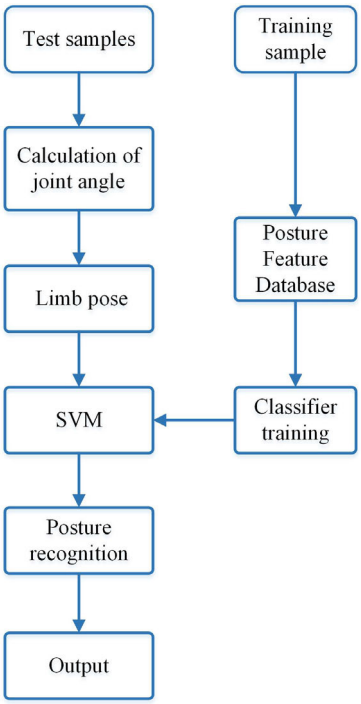

FIGURE 7. Flow chart of the lying posture recognition algorithm.

Because human posture samples are multidimensional and nonlinear, we use a nonlinear kernel function to simplify the inner product operations in the mapping space and map the nonlinear training data to a higher dimensional space. The Gauss kernel function is a nonlinear function. Due to its wide convergence, the Gauss kernel function can be applied regardless of the dimension and sample size [39]. In this paper, the Gauss kernel function is used as the kernel function of the SVM as follows:

$$K(x, x_i) = \exp\left(-\frac{\|x - x_i\|^2}{2\sigma^2}\right) \tag{11}$$

where $K(x, x_i)$ is the kernel function and σ is the width parameter of the kernel function, which determines the generalization scale of the kernel function.

B. TRAINING

The SVM is trained utilizing the postures of the limbs and the lying postures to obtain the classifier model. In Table 3, the 9 postures of the left upper limb are abbreviated as LUO, LUT, LUH, LUF, LUI, LUS, LUE, LUG, and LUN, and the waist has 2 postures, abbreviated as WON and WTW. The abbreviations of the other limb postures indicate a certain posture of a certain limb, as shown in Table 3 below.

In this work, we used the Kinect camera to collect human skeleton information. The Kinect sensor is able to recognize the 3D position of 25 body joints at a 30-Hz imaging speed. The camera uses visual and infrared sensors to acquire color images and depth image sequences of human motion through OpenNI and then uses the NiTE middleware-based development kit to track the position of the joints in the Kinect coordinate system in real time [40]. With WIN7, Visual Studio 2012, and Kinect for Windows SDK, we extracted the space coordinates of human joints through the C++ program.

V. EXPERIMENT

A. DATASET

The human in-bed posture data used in the study are collected from a hospital and a laboratory (Fig. 8.). The 32 participants (16 males and 16 females) aged from 21 to 57. The data were collected by a Kinect camera (Kinect v2), and, each experiment was performed 10 times by 32 subjects; a total of 19,800 human lying in-bed depth images were obtained. The advantages of the experiment include the following. (1) Each lying posture was conducted by 32 participants to reduce individual differences. (2) Each participant repeatedly conducted the same set of lying postures, but we asked participants to slightly change the limb postures to ensure the integrity of the data and the breadth of the samples. Compared with the currently published in-bed datasets [8], [15], [26], our dataset collected by visual camera including the depth and RGB images is unique based on the fine-grained postures that contain almost all limb movement ranges. Our dataset can recognize 20 fine-grained lying postures.

B. RESULTS

The dataset is divided into a training set and a test set at the ratio of 6:4. The data sources of the training set and test set are from different participants, i.e., the training set data are from the participants labeled 1-20, and the test set data are from the participants labeled 21-32.

The accuracy of each posture and the overall accuracy are shown in Table 4. An overall accuracy of 97.1% was achieved on our dataset. Among the 20 lying postures recognized

FIGURE 8. Collection of human lying posture data. (a) data collected from a hospital, (b) data collected in the laboratory.

TABLE 4. The accuracies (%) of different postures and overall.

Actual	Predicted Human Posture																			Accuracy	Overall
Posture	P1	P2	P3	P4	P5	P6	P7	P8	P9	P10	P11	P12	P13	P14	P15	P16	P17	P18	P19	P20	(%)	(%)
P1	**98.33**		0.83		0.83																98.33	
P2	0.83	**99.17**		0.83	0.83																99.17	
P3			**97.5**		2.5			0.83													97.5	
P4				**96.67**			0.83														97.67	
P5		0.83	0.83		**94.17**																94.17	
P6	0.83		0.83	1.67		**99.17**				0.83											99.17	
P7				0.83	0.83	0.83	**97.5**				0.83										97.5	
P8								**92.5**						1.67							92.5	
P9					0.83		0.83		**99.17**		0.83		0.83								99.17	
P10								0.83		**96.67**							0.83				96.67	97.1
P11								0.83		1.67	**96.67**				0.83						96.67	
P12							0.83		0.83		0.83	**99.17**	0.83	0.83		0.83	0.83				99.17	
P13													**97.5**								97.5	
P14								4.17		0.83				**96.67**	0.83	0.83		0.83			96.67	
P15											0.83		0.83		**94.17**		3.33			0.83	94.17	
P16								0.83								**98.33**		0.83			98.33	
P17												0.83			3.33		**93.33**		0.83		93.33	
P18														0.83			0.83	**97.5**		0.83	97.5	
P19																	0.83	0.83	**99.17**	0.83	99.17	
P20															0.83					**97.5**	97.5	

as shown in Table 4, the accuracy of postures 2, 6, 9, 12 and 19 reached 99.17%. However, lower accuracy was exhibited in the recognition of postures 3, 5, 8, 14, 15 and 17. Moreover, there are certain common characteristics in these misrecognized categories. Posture 5 was incorrectly recognized as posture 3. Posture 8 was incorrectly recognized as posture 14 and vice-versa. Posture 15 was recognized as posture 17 and vice-versa. The reason for these errors is mainly because these postures are very similar to each other. More concretely, lying postures 8 and 14 are similar postures and lying postures 15 and 17 are also similar.

C. COMPARISON WITH RELATED WORKS

Due to different purposes, previous research has mainly focused on the recognition of several classes of lying postures: three postures, four postures, five postures,

TABLE 5. Accuracy (%) comparison with related works.

Author name	Sensor type	Classification method	Number of postures	Accuracy (%)
T. Harada *et al.* [13]	Pressure Matrix + Video camera	Model-based pressure image templates	3	—
H.M. Clever *et al.* [15]	Pressure Matrix	ConvNets	3D posture	—
M. Heydarzadeh et al. [11]	Pressure Matrix	GMM + k-NN	3	98.1
R. Grimm *et al.* [14]	Pressure Matrix	k-NN	4	95.5
	Range imaging			79.4
Y. Enokibori *et al.* [41]	Pressure Matrix	DNN	4	97.1
G. Matar *et al.* [12]	Pressure Matrix	FFANN	4	97.9
R. Yousefi *et al.* [9]	Pressure Matrix	PCA + k-NN	5	97.7
C. C. Hsia *et al.* [18]	Pressure Matrix	RawData + SVM	6	83.5
J. J. Liu *et al.* [19]	Pressure Matrix	Minimum class residual	6	83.2
M. B. Pouyan *et al.* [10]	Pressure Matrix	Hamming distance similarity + k-NN	8	97.1
W. Huang *et al.* [27]	Pressure Matrix + Video camera	PCA + SVM	9	94.1
Vision-based lying posture recognition method				
Mondragon *et al.* [43]	Kinect v2	CNN-SkelPose	Upper-body skeleton estimation	—
T. Harada *et al.* [13]	Pressure Matrix + Video camera	Model-based pressure image templates	3	—
S. Liu *et al.* [26]	IR + RGB camera	Stacked hourglass network	3	98
W. Huang *et al.* [27]	Pressure Matrix + Video camera	PCA + SVM	9	94.1
This paper	**Kinect v2**	**Fuzzy + SVM**	**20**	**97.1**

six postures, eight postures, and nine postures. To the best of our knowledge, so far, no study has focused on the same fine-grained posture recognition, such as 20 lying postures, as we have in this study. Therefore, we cannot carry out a fair comparison of similar capabilities and posture granularity. However, to make an effective comparison, the results of this paper were compared with related studies on posture categories and methods. The comparison is summarized in Table 5. The comparisons show the data efficiency of the method proposed in this paper and the reliable accuracy for fine-grained human lying posture recognition.

As DCNNs and big data science are advancing rapidly, deep learning is playing an increasingly important role in computer vision and image processing. Liu *et al.* proposed a new idea using a shallow dataset collected from lying postures to fine-tune a CNN, which was pretrained on large public datasets, and the application of deep learning in the recognition of human postures in-bed is a meaningful quest [18]. At present, the size of the existing in-bed dataset is not large enough to support DCNN training for fine-grained posture classification. Because the size of the in-bed dataset is small and it is difficult to collect more data, it has always been our effort to increase the efficiency of the data and the resources. Therefore, the proposed method achieved a high data efficiency and high classification accuracy in recognizing human in-bed lying postures.

VI. CONCLUSION

This paper presented an approach that can accurately and efficiently recognize 20 different human in-bed lying postures using a Kinect sensor and a fuzzy-logic and machine-learning combined algorithm. The intention of the research was to

allow an assistive robot or another automated healthcare system to recognize the body-limb posture of a patient lying in bed for automated healthcare service. The work made the following three new contributions:

(1) A new human lying posture dataset was created and released to the research community. This whole-body lying posture dataset was obtained by labeling the images of the limb postures and the whole-body lying postures. The dataset can be used to train a classifier for identifying a person's in-bed lying posture among 20 possible postures.

(2) Based on the depth images and the skeleton data in the dataset, a set of fuzzy rules was obtained by analyzing the samples of the whole-body lying postures. Then, a relational model between the joint angles and the limb postures was obtained to recognize limb postures through the posture recognition process.

(3) Data efficient posture classification was achieved by using the proposed method with an accuracy rate of 97.1%. The verification experiment showed that random lying postures can be recognized and that the recognized lying postures coincide with the actual postures, which meets our goal of recognizing dynamic or static postures in real time.

Although we tested the presented method using SVM as the classification tool, it can be reasonably anticipated that other machine learning algorithms would also work. A comparative study of performance using different machine learning algorithms will be a future work.

ACKNOWLEDGMENT

The authors would like to thank the Rehabilitation Medicine Department, China-Japan Friendship Hospital, for supporting the experiments and data collection in this study, which made this research possible.

REFERENCES

[1] A. Bilyea, N. Seth, S. Nesathurai, and H. A. Abdullah, "Robotic assistants in personal care: A scoping review," *Med. Eng. Phys.*, vol. 49, pp. 1–6, Nov. 2017.

[2] D. Park, Y. Hoshi, H. P. Mahajan, H. K. Kim, Z. Erickson, W. A. Rogers, and C. C. Kemp, "Active robot-assisted feeding with a general-purpose mobile manipulator: Design, evaluation, and lessons learned," *Robot. Auto. Syst.*, vol. 124, Feb. 2020, Art. no. 103344.

[3] P. M. Grice and C. C. Kemp, "In-home and remote use of robotic body surrogates by people with profound motor deficits," *PLoS ONE*, vol. 14, no. 3, Mar. 2019, Art. no. e0212904.

[4] P. M. Grice and C. C. Kemp, "Assistive mobile manipulation: Designing for operators with motor impairments," in *Proc. RSS Workshop Socially Phys. Assistive Robot. Hum.*, 2016, pp. 1–8.

[5] H.-S. Kim, C.-H. Park, D.-I. Park, H.-M. Do, T.-Y. Choi, D.-H. Kim, and J.-H. Kyung, "Design of high payload dual arm robot with modifiable forearm module depending on mission," in *Proc. 14th Int. Conf. Ubiquitous Robots Ambient Intell. (URAI)*, Jun. 2017, pp. 83–84.

[6] L. Yan, Z. Mu, W. Xu, and B. Yang, "Coordinated compliance control of dual-arm robot for payload manipulation: Master-slave and shared force control," in *Proc. IEEE/RSJ Int. Conf. Intell. Robots Syst. (IROS)*, Oct. 2016, pp. 2697–2702.

[7] S. Ostadabbas, R. Yousefi, M. Nourani, M. Faezipour, L. Tamil, and M. Pompeo, "A posture scheduling algorithm using constrained shortest path to prevent pressure ulcers," in *Proc. IEEE Int. Conf. Bioinf. Biomed.*, Nov. 2011, pp. 327–332.

[8] M. B. Pouyan, J. Birjandtalab, M. Heydarzadeh, M. Nourani, and S. Ostadabbas, "A pressure map dataset for posture and subject analytics," in *Proc. IEEE EMBS Int. Conf. Biomed. Health Informat. (BHI)*, Feb. 2017, pp. 65–68.

[9] R. Yousefi, S. Ostadabbas, M. Faezipour, M. Farshbaf, M. Nourani, L. Tamil, and M. Pompeo, "Bed posture classification for pressure ulcer prevention," in *Proc. Annu. Int. Conf. IEEE Eng. Med. Biol. Soc.*, Aug. 2011, pp. 7175–7178.

[10] M. B. Pouyan, S. Ostadabbas, M. Farshbaf, R. Yousefi, M. Nourani, and M. D. M. Pompeo, "Continuous eight-posture classification for bed-bound patients," in *Proc. 6th Int. Conf. Biomed. Eng. Informat.*, Dec. 2013, pp. 121–126.

[11] M. Heydarzadeh, M. Nourani, and S. Ostadabbas, "In-bed posture classification using deep autoencoders," in *Proc. 38th Annu. Int. Conf. IEEE Eng. Med. Biol. Soc. (EMBC)*, Aug. 2016, pp. 3839–3842.

[12] G. Matar, J.-M. Lina, and G. Kaddoum, "Artificial neural network for in-bed posture classification using bed-sheet pressure sensors," *IEEE J. Biomed. Health Informat.*, vol. 24, no. 1, pp. 101–110, Jan. 2020.

[13] T. Harada, T. Mori, Y. Nishida, T. Yoshimi, and T. Sato, "Body parts positions and posture estimation system based on pressure distribution image," in *Proc. IEEE Int. Conf. Robot. Autom.*, vol. 2, May 1999, pp. 968–975.

[14] R. Grimm, S. Bauer, J. Sukkau, J. Hornegger, and G. Greiner, "Markerless estimation of patient orientation, posture and pose using range and pressure imaging," *Int. J. Comput. Assist. Radiol. Surgery*, vol. 7, no. 6, pp. 921–929, Nov. 2012.

[15] H. M. Clever, A. Kapusta, D. Park, Z. Erickson, Y. Chitalia, and C. C. Kemp, "3D human pose estimation on a configurable bed from a pressure image," in *Proc. IEEE/RSJ Int. Conf. Intell. Robots Syst. (IROS)*, Oct. 2018, pp. 54–61.

[16] A. Kapusta, P. Grice, H. Clever, Y. Chitalia, D. Park, and C. Kemp, "A system for bedside assistance that integrates a robotic bed and a mobile manipulator," *PLoS ONE*, vol. 14, Oct. 2019, Art. no. e0221854.

[17] L. Casas, N. Navab, and S. Demirci, "Patient 3D body pose estimation from pressure imaging," *Int. J. Comput. Assist. Radiol. Surg.*, vol. 14, no. 3, pp. 517–524, Mar. 2019.

[18] C. C. Hsia, K. J. Liou, A. P. W. Aung, V. Foo, W. Huang, and J. Biswas, "Analysis and comparison of sleeping posture classification methods using pressure sensitive bed system," in *Proc. Annu. Int. Conf. IEEE Eng. Med. Biol. Soc.*, Sep. 2009, pp. 6131–6134.

[19] J. J. Liu, W. Xu, M.-C. Huang, N. Alshurafa, M. Sarrafzadeh, N. Raut, and B. Yadegar, "Sleep posture analysis using a dense pressure sensitive bedsheet," *Pervas. Mobile Comput.*, vol. 10, pp. 34–50, Feb. 2014.

[20] A. Sadeh and C. Acebo, "The role of actigraphy in sleep medicine," *Sleep Med. Rev.*, vol. 6, no. 2, pp. 113–124, May 2002.

[21] G. Matar, J.-M. Lina, J. Carrier, and G. Kaddoum, "Unobtrusive sleep monitoring using cardiac, breathing and movements activities: An exhaustive review," *IEEE Access*, vol. 6, pp. 45129–45152, 2018.

[22] J.-R. Ding, "Bed status detection for elder-care center," in *Proc. 16th Int. Conf. Syst., Signals Image Process.*, Jun. 2009, pp. 1–4.

[23] J. Shotton, A. Fitzgibbon, M. Cook, T. Sharp, M. Finocchio, R. Moore, A. Kipman, and A. Blake, "Real-time human pose recognition in parts from single depth images," in *Proc. CVPR*, Jun. 2011, pp. 1297–1304.

[24] F. Achilles, A.-E. Ichim, H. Coskun, F. Tombari, S. Noachtar, and N. Navab, "Patient MoCap: Human Pose Estimation Under Blanket Occlusion for Hospital Monitoring Applications," in *Medical Image Computing and Computer-Assisted Intervention—MICCAI*. Cham, Switzerland: Springer, 2016, pp. 491–499.

[25] M.-C. Yu, H. Wu, J.-L. Liou, M.-S. Lee, and Y.-P. Hung, "Multiparameter Sleep Monitoring Using a Depth Camera," in *Biomedical Engineering Systems and Technologies*. Berlin, Germany: Springer, 2013, pp. 311–325.

[26] S. Liu and S. Ostadabbas, "Seeing under the cover: A physics guided learning approach for in-bed pose estimation," in *Proc. 22nd Int. Conf. Med. Image Comput. Comput. Assist. Intervent. (MICCAI)*, Shenzhen, China, Oct. 2019, pp. 236–245.

[27] W. Huang, A. A. P. Wai, S. F. Foo, J. Biswas, C.-C. Hsia, and K. Liou, "Multimodal sleeping posture classification," in *Proc. 20th Int. Conf. Pattern Recognit.*, Aug. 2010, pp. 4336–4339.

[28] C.-H. Kuo, F.-C. Yang, M.-Y. Tsai, and M.-Y. Lee, "Artificial neural networks based sleep motion recognition using night vision cameras," *Biomed. Eng., Appl., Basis Commun.*, vol. 16, no. 2, pp. 79–86, Apr. 2004.

[29] W. Gong, X. Zhang, J. Gonzàlez, A. Sobral, T. Bouwmans, C. Tu, and E.-H. Zahzah, "Human pose estimation from monocular images: A comprehensive survey," *Sensors*, vol. 16, no. 12, p. 1966, Nov. 2016.

[30] N. Sarafianos, B. Boteanu, B. Ionescu, and I. A. Kakadiaris, "3D human pose estimation: A review of the literature and analysis of covariates," *Comput. Vis. Image Understand.*, vol. 152, pp. 1–20, Nov. 2016.
[31] C. Cornelis, G. Deschrijver, and E. E. Kerre, "Advances and challenges in interval-valued fuzzy logic," *Fuzzy Sets Syst.*, vol. 157, no. 5, pp. 622–627, Mar. 2006.
[32] M. Alenezi, A. Agrawal, R. Kumar, and R. A. Khan, "Evaluating performance of Web application security through a fuzzy based hybrid multicriteria decision-making approach: Design tactics perspective," *IEEE Access*, vol. 8, pp. 25543–25556, 2020.
[33] M. H. Homaei, F. Soleimani, S. Shamshirband, A. Mosavi, N. Nabipour, and A. R. Varkonyi-Koczy, "An enhanced distributed congestion control method for classical 6LowPAN protocols using fuzzy decision system," *IEEE Access*, vol. 8, pp. 20628–20645, 2020.
[34] J. Kurosu, A. Yorozu, and M. Takahashi, "Simultaneous dual-arm motion planning considering shared transfer path for minimizing operation time," in *Proc. 11th Asian Control Conf. (ASCC)*, Dec. 2017, pp. 467–472.
[35] M. A. MacConaill"The movements of bones and joints; the mechanical structure of articulating cartilage," *J. Bone Joint Surg. Brit. Volume*, vol. 33B, no. 2, p. 251, 1951.
[36] P. Neamatollahi, M. Hadi, and M. Naghibzadeh, "Simple and efficient pattern matching algorithms for biological sequences," *IEEE Access*, vol. 8, pp. 23838–23846, 2020.
[37] Z. Zhao, Y. Song, F. Cui, J. Zhu, C. Song, Z. Xu, and K. Ding, "Point cloud features-based kernel SVM for human-vehicle classification in millimeter wave radar," *IEEE Access*, vol. 8, pp. 26012–26021, 2020.
[38] R. Debnath, N. Takahide, and H. Takahashi, "A decision based one-against-one method for multi-class support vector machine," *Pattern Anal. Appl.*, vol. 7, no. 2, pp. 164–175, Jul. 2004.
[39] J. Cao, G. Lv, C. Chang, and H. Li, "A feature selection based serial SVM ensemble classifier," *IEEE Access*, vol. 7, pp. 144516–144523, 2019.
[40] Y. Li, L. Berkowitz, G. Noskin, and S. Mehrotra, "Detection of patient's bed statuses in 3D using a microsoft Kinect," in *Proc. 36th Annu. Int. Conf. IEEE Eng. Med. Biol. Soc.*, Aug. 2014, pp. 5900–5903.
[41] Y. Enokibori and K. Mase, "Data augmentation to build high performance DNN for in-bed posture classification," *J. Inf. Process.*, vol. 26, pp. 718–727, Oct. 2018.
[42] L. A. Zavala-Mondragon, B. Lamichhane, L. Zhang, and G. D. Haan, "CNN-SkelPose: A CNN-based skeleton estimation algorithm for clinical applications," *J. Ambient Intell. Hum. Comput.*, vol. 11, no. 6, pp. 2369–2380, Jun. 2020.

WEIYAN REN (Graduate Student Member, IEEE) received the B.S. and M.S. degrees from the China University of Petroleum, Beijing, China, in 2014 and 2017, respectively. He is currently pursuing the Ph.D. degree in robotics with Tsinghua University, Beijing. His research interests include intelligent control of robotic systems, human–machine interaction and collaboration, and deep learning. His awards and honors include the National Scholarship for undergraduates, the National Scholarship for master's, the Comprehensive First-Class Scholarships, and the Innovative First-Class Scholarships.

OU MA received the Ph.D. degree from McGill University, in 1991.

He is currently the Alan B. Shepard Chair Professor with the Department of Aerospace Engineering and Engineering Mechanics, University of Cincinnati. He worked at MDA Space Missions (then Spar Aerospace Ltd.), from 1991 to 2002, participated in the development of the International Space Station (ISS) robotic systems, SSRMS, and SPDM, and led several research and development projects for developing modeling, simulation, and verification technologies for the two ISS robots. He worked at New Mexico State University as an Associate Professor, from 2002 to 2008; a Professor, from 2008 to 2012; and the Chair Professor, from 2012 to 2017, where he developed three research laboratories and led many research projects regarding nonlinear control, contact dynamics, and human body modeling and simulation. He has coauthored over 150 peer-reviewed publications. His current research interests include intelligent control of robotic systems, human–robot and robot–robot interaction and collaboration, and smart manufacturing.

HONGXIN JI was born in Shandong, China, in 1988. He received the B.S. degree in electrical engineering from Shandong Agriculture University, in 2010, and the Ph.D. degree in electrical engineering from North China Electric Power University, Beijing, China, in 2017. He is currently undertaking a Postdoctoral Research with the School of Aerospace Engineering, Tsinghua University, Beijing. His current research interests include electrical insulation and materials, condition monitoring of power apparatus and cooperative motion planning, and control of dual-arm robot.

XINYUAN LIU (Member, IEEE) received the bachelor's degree from the Beijing University of Chinese Medicine, in 2017, where he also received the direct Ph.D. opportunity, in 2017. He is currently pursuing the Ph.D. degree.

From 2012 to 2017, he specialized in traditional Chinese medicine and studied at the First Affiliated Hospital, Beijing University of Chinese Medicine. The professional direction of the doctoral stage is integrated Chinese and western medicine. He followed the instructor in the standardized training of residents at the China-Japan Friendship Hospital. He is the author of four Chinese books. He has participated in publishing three SCI articles and 15 Chinese articles. His research interest includes the application of a combination of traditional Chinese and western medicine to the treatment of functional gastrointestinal and chronic liver diseases. His current research interests include randomized controlled clinical trial of traditional Chinese medicine and vegetarian therapy for functional constipation. He received the School-Level Scholarships and the Chinese Medicine Communication Scholarships.